COMBINING FINGERPRINT, PALMPRINT AND HAND-SHAPE FOR USER AUTHENTICATION

Ajay Kumar[1,2], *David Zhang*[1]

[1]Department of Computing
The Hong Kong Polytechnic University, Hong Kong.

[2]Department of Electrical Engineering
Indian Institute of Technology Delhi, New Delhi, India.

Email: ajaykr@ieee.org, csdzhang@comp.polyu.edu.hk

ABSTRACT

This paper investigates a new approach for personal authentication by combining unique biometric features which can be acquired from hand images alone. The proposed method attempts to improve the performance of fingerprint-based verification system by integrating palmprint and hand-shape features. The matching scores for the fingerprint images are computed using the number of matched minutiae on the overlapping areas while those for palmprint and hand-shape images are based on distance of feature vectors. These matching scores are combined using simple fusion rule which does not require any training. Our experimental results on the database of 100 users achieve promising results and therefore confirm the usefulness of proposed method.

1. INTRODUCTION

The Primary objective of any biometric authentication system [7] is to achieve higher performance while utilizing most of the discriminant features. The fingerprint, palmprint and hand shape can be simultaneously extracted from a typical hand image. The nature of features (minutiae) traditionally employed for the fingerprint matching requires a high resolution fingerprint image which is higher than those required for palmprint or hand shape. However, the simultaneous acquisition of such fingerprint images is not difficult and can be achieved with the usage fingerprint sensor focusing on thumb/finger.

The acquisition of hand images that can deliver palmprint and hand-shape information is easy and has been demonstrated in our earlier work [4]-[5]. In the context of recent work in [4] and the current popularity of multimodal system, this assertion that fingerprints could offer improved performance while integrating with palmprint and hand-shape, deserves careful evaluation. The experiments reported in this paper are aimed at investigating the performance improvement for such multimodal system for which all the three modalities can be acquired at once.

The block diagram of the proposed hand-based biometric authentication system is shown in Figure 1. The hand images acquired from the digital camera are used to extract two distinct images: (i) binary image depicting hand shape, and (ii) gray-level region of interest (ROI) depicting palmprint texture. The method of extracting these two images is same as reported in earlier study [4]. The fingerprint images can also be acquired simultaneously and assumed here as another output from the hand imaging device. The matching scores from the palmprint, fingerprint, and hand-shape images, with those stored during registration, are used to generate the combined matching score. This combined matching score is used to authenticate a user in one of the two classes, *i.e.* genuine or imposter. The details of feature extraction and computation of matching score, for each of the three modalities, is described in the following section.

2. FINGERPRINT MATCHING

Each of the fingerprint images are firstly enhanced the ridges and reduce the noise. The enhancement is done by determining the irregular regions in the image. The image is then binarized and rotated as per the ridge flows of the fingerprint. The fingerprint enhancement and matching method employed in this work is similar as detailed in [2] and [1] respectively. As shown in figure 2, after the enhancement of the image has been completed, the minutiae in the image are located and for each of the detected minutiae a three-tuple primary feature is created which contains the x and y co-ordinates of the minutia along with the relative angle of the minutia. Also for each minutia a five-tuple secondary vector is created which contains the Euclidian distance of the minutia from its two nearest neighbors, along with the orientation difference between the central minutia and the two neighbors; and it also contains the acute angle between the radial lines from the central minutia. The nearest neighbors are not calculated on the basis of their Euclidian distance from the central minutia but are based on the following criteria;

$$\left| N_0 M_i \times N_1 M_i \right| \geq 0 \qquad (1)$$

where, N_i are the neighboring minutiae of the central minutia. This method increases the chances of flipping the order of the minutiae.

The next step is feature matching. Here there could be three possible cases with regard to the number of the minutiae detected in both the images. The first case is when the number of minutiae in both images is less than the decided threshold value. The next case is when the number of minutiae in one of the images is less than the threshold value. The final case is when the number of minutiae detected in both the images is greater than the threshold.

In the first and second cases, we match all the feature points directly by forcing a matching process on all possible cases of matching. Thus all possible matching features are tabulated. The process is generally termed as 'forced' Matching since there are no criteria in deciding which two features need to be compared. This method is however quite computationally expensive and crude in approach since no intelligence has been used. However in the third case, the cost of forced matching is much higher than what can be handled. So here we use the secondary features to calculate the matching feature pairs. Here we first calculate a list of all the possible matches that could exist for each minutia and then obtain the most optimum using the minimum cost flow graph. Thus we can create a set of matched features.

In the case of the use of secondary features being used for matching, there is a problem in that the feature vectors only tell about the local structure of the minutia and not about its global structure. In order to resolve such problems, a validation step is applied by requiring that all the matched feature pairs should have similar orientation differences if they come in the same finger. It is done by creating an orientation difference and plotting the histogram for each bin. The matching score is computed using the number of matched minutiae on overlapping areas and the average feature distances. This matching score is used in the fusion and decision stages.

3. HAND-SHAPE MATCHING

Hand shape representation requires effective and perceptually important features based on geometrical information or geometry plus interior content. In this work we extracted 17 features to characterize every hand-shape images; *i.e.* perimeter, 4 finger length, 8 finger width, palm width, palm length, hand area, and hand length (also detailed in [4]). The distance between feature vector from an unknown hand shape *f* and that from the known class *j* is computed from the Euclidean norm ($\|.\|$) *i.e.*,

$$h(f, f_j) = \left\| f^i - f_j^i \right\| \quad (2)$$

The fingerprint and palmprint matching scores are further consolidated with the distance measure $h(f, f_j)$ and this is detailed in section 5.

4. PALMPRINT MATCHING

The palmprint pattern is mainly made up of palm lines, *i.e.*, principal lines and creases. Palmprint matching using line features is reported to be powerful and offers high accuracy in palmprint verification. Significant line features from the normalized palmprint images are detected using four line detectors or directional masks. Each of these masks can detect lines oriented at 0^o (h_1), 45^o (h_2), 90^o (h_3), and 135^o (h_4). The spatial extent of these masks was empirically fixed as 9×9. Each of these masks is used to filter the normalized palmprint images as follows:

$$J_1(x, y) = h_1 * J'(x, y) \quad (3)$$

where '*' denotes the discrete 2D convolution. Thus four filtered images, *i.e.*, $J_1(x, y), J_2(x, y), J_3(x, y)$ and $J_4(x, y)$, from each of the masks h_1, h_2, h_3 and h_4 respectively, are obtained. The final image $J_f(x, y)$ is generated as follows [4]:

$$J_f(x, y) = \max_{(x,y) \in J} \{J_1(x, y), J_2(x, y), J_3(x, y), J_4(x, y)\} \quad (4)$$

The resultant image represents the combined directional map of palm-lines in the palmprint image $J(x, y)$. The image pixels in $J_f(x, y)$ can be efficiently characterized by the localized estimation of statistical moments. For computational reasons, we used standard deviation to compute the localized palmprint features. The image $J_f(x, y)$ is divided into a set of *n* overlapping blocks and standard deviation of pixels in each of these overlapping blocks is used to form the feature vector.

$$v_{palm} = \{\sigma_1, \sigma_2, \ ..., \sigma_n\} \quad (5)$$

where σ_1 is the standard deviation in the overlapping first block. The palmprint images from every user is characterized by feature vector v_{palm} and used for identification. The cosine similarity measure is used to compute the distance between the feature vector *f* and that from unknown class *j*, *i.e.*,

$$p(f, f_j) = 1 - \frac{f^T . f_j}{\|f\| . \|f_j\|} \quad (6)$$

While matching the unknown feature vector f_j with the ones from the training samples, the minimum of similarity measure is assigned as the final matching distance.

5. EXPERIMENTS & RESULTS

In order to examine the goals of our experiments the image database from 100 users was employed. The image acquisition setup using a digital camera was employed to collect 8 images per user. These hand images were collected during a period of about two months, as the goal of experiments was to investigate the fusion of biometric modalities instead of their stability with time. The preprocessing described in earlier study [4] was used to obtain palmprint and hand shape images. The size of each of the segmented gray-level image was 300×300 pixels. Each of these images was divided into 24×24 pixels with an overlapping of 6 pixels. The feature vector of size 1×23 from hand shape and 1×144 from the palmprint image

was used to evaluate the performance. The fingerprint images from the FVC2004 DB2 database [3] which are composed of 8 images from each of 100 users were employed. Each of these fingerprint images were randomly paired† [6] with hand images (palmprint and hand-shape images) to obtain a three image set for every user. The matching scores for the fingerprint images were computed as detailed in section 2. The individual matching scores from the fingerprint, palmprint and hand-shape were combined using sum rule. The first image sample for every user was used for the registration and remaining seven images were used as independent test data.

Figure 5 shows the genuine and imposter distribution of test data from the fingerprint, palmprint and hand-shape images. The receiver operating characteristics (ROC) from the test data is displayed in figure 6. The performance improvement due to the simultaneous usage of three images, *i.e.* fingerprint, palmprint and hand-shape, can be visualized in this figure. The individual ROC for fingerprint, palmprint and hand-shape is also displayed in the figure 6. The quantitative performance corresponding to each of the case in Figure 6 is shown in Table 1. The parameters of total minimum error, along with their respective decision threshold and Equal Error Rate (*EER*) are displayed in this Table. The performance score from each of these cases can also be ascertained by criterion J [8];

$$J = \frac{(\mu_g - \mu_i)^2}{\sigma_g^2 + \sigma_i^2} \qquad (7)$$

where μ_g, μ_i are the mean and σ_g, σ_i are the standard deviation of genuine and impostor distributions respectively. It can be noticed from table 1 that the The utility of combining fingerprint with palmprint and hand-shape is can be ascertained from the large improvement in the performance scores (*J*) as illustrated in table 1. The significant reduction in error rates, *i.e.* total minimum error, as compared to those achieved by fingerprint, palmprint or hand-shape alone can also be observed from this table.

7. CONCLUSIONS AND FUTURE WORK

The objective of this work was to investigate the integration of fingerprint with palmprint and hand-shape features to achieve higher accuracy in fingerprint-based authentication systems. The results shown in table 1 and figure 5 demonstrate that this is indeed the case. The results should be interpreted in the context of low quality fingerprint images from FVC 2004 database; further improvement in the combined performance, when the images are acquired from a live fingerprint sensor, is intuitively expected. The experimental results reported in this paper are preliminary as we are working to acquire a large database in which the fingerprint images are also acquired using live sensor (from the same hands used for the palmprint and hand-shape extraction). The main problem in the usage of the proposed system lies in the imaging of fingerprints while the user is positioning himself/herself for the acquisition of hand images. However, the implementation of such imaging setup, which can simultaneously capture fingerprint region with high resolution (500 dpi), is certainly possible and is suggested for future work.

† The mutual independence of biometric modalities allows us to argument two biometric indicators that are collected individually.

8. REFERENCES

[1] T.-Y. Jea and V. Govindaraju, "A minutia-based partial fingerprint recognition system," *Pattern Recognition*, vol. 38, pp. 1672-1684, 2005.

[2] L. Hong, Y. Wan and A.K. Jain, "Fingerprint Image Enhancement: Algorithms and Performance Evaluation", *IEEE Trans. Patt. Anal. Machine Intell.*, vol. 20, pp. 777-789, Aug. 1998.

[3] http://bias.csr.unibo.it/fvc2004

[4] A. Kumar, D. C. M. Wong, H. C. Shen, and A. K. Jain, "Personal verification using palmprint and hand geometry biometric," *Proc. AVBPA 2003*, pp. 668-675, 2003.

[5] A. Kumar and D. Zhang, "Personal recognition using hand-shape and texture," to appear in *IEEE Trans. Image Processing*, Jul. 2006.

[6] A. Ross, A. K. Jain, J.-Z. Qian, "Information fusion in biometrics," *Pattern Recognition Lett.*, vol. 24, pp. 2115-2125, Sep. 2003.

[7] S. Z. Li, J. Lai, T. Tan, G. Feng, Y. Wang (eds.). *Advances in Biometric Authentication*. Springer, 2004.

[8] A. Kumar and G. Pang, "Defect detection in textured materials using optimized filters," *IEEE Trans. Systems, Man, and Cybernetics : Part B, Cybernetics*, vol. 32, no. 5, pp. 553-570, Oct. 2002

Table 1: Performance indices from individual feature sets and from the fusion of matching scores.

Modalities	Total Minimum Error				
	FAR	*FRR*	Threshold	*EER*	*J*
Hand Shape	3.79	10.71	0.0687	8.504	1.284
Palmprint	3.906	16.85	0.970	11.06	1.914
Fingerprint	11.71	0.00	0.0185	11.4	1.18
Hand Shape + Palmprint	1.929	10.28	0.9082	7.15	2.813
Hand Shape + Palmprint + Fingerprint	5.01	0.601	0.6143	3.53	3.786

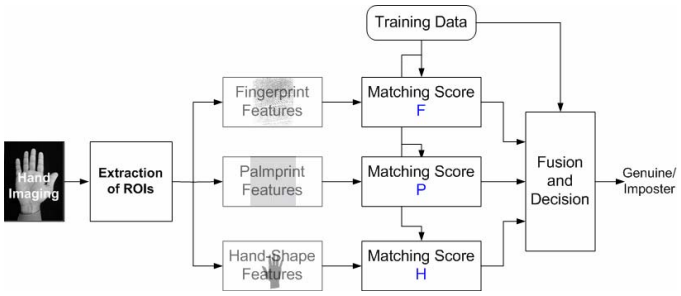

Figure 1: Block diagram of the proposed personalα authentication system.

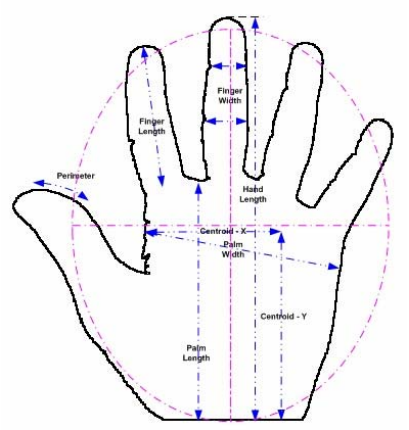

Figure 2: Hand-shape features extracted from the hand images.

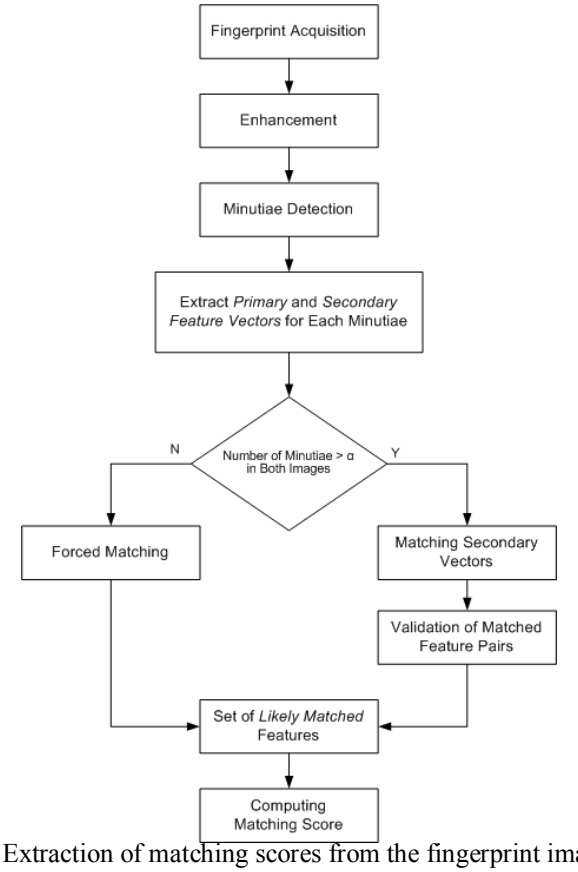

Figure 3: Extraction of matching scores from the fingerprint images.

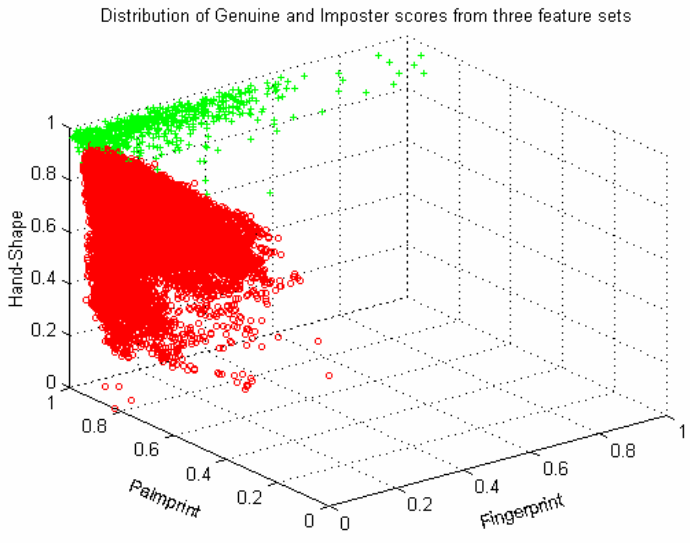

Figure 4: Distribution of genuine (+) and imposter (o) matching scores.

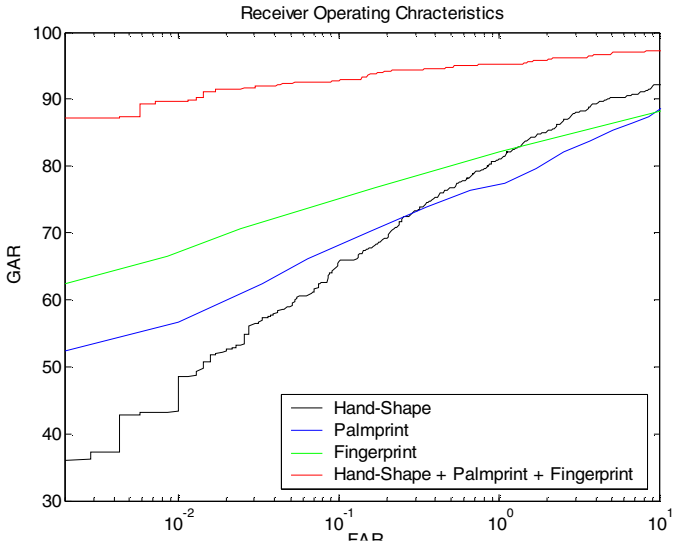

Figure 5: The comparative ROC from the test data in experiments.